Astron. Astrophys. 344, 779–786 (1999)

ASTRONOMY AND ASTROPHYSICS

The 10 GHz–10 THz spectrum of a normal spiral galaxy

J. Braine[1] **and D.H. Hughes**[2,3]

[1] Observatoire de Bordeaux, UMR 5804, CNRS/INSU, B.P. 89, F-33270 Floirac, France
[2] Institute for Astronomy, University of Edinburgh, Royal Observatory, Blackford Hill, Edinburgh, EH9 3HJ, UK
[3] INAOE, Apartado Postal 51 y 216, 72000 Puebla, Pue., Mexico

Received 5 May 1998 / Accepted 21 January 1999

Abstract. We present a complete FIR spectral energy distribution of a normal spiral disk. A full grating scan, from 43–189 μm, centered on the nucleus of NGC 4414 was made with the ISO Long Wavelength Spectrometer (LWS). The mid-IR to millimeter continuum of NGC 4414 can be modeled with thermal dust emission from a warm component at 69 K and a cool component at 24.5 K. At a distance of 9.6 Mpc, the LWS beam samples only the central ≈ 4 kpc, which includes most of the FIR-bright disk but excludes dust emission from a cooler phase of the ISM in the outer regions of the galaxy (e.g. $T \lesssim 20\,\mathrm{K}$ at $r > 2\,\mathrm{kpc}$). The emission we detect comes from the inner disk ($4'' \gtrsim r \gtrsim 40''$) rather than the nucleus, which is poor in ionized and neutral gas. Three important cooling lines of the ISM, CII(158 μm), NII(122 μm), and OI(63 μm) are strong and a weak OIII(88 μm) line is detected as well. OI(146 μm) is weak or not detected. No detections were found for OIII(52 μm) and NIII(57 μm). With a spectral resolution of $\sim 1500\,\mathrm{km\,s^{-1}}$ (FWHM) in grating-scan mode, LWS was unable to resolve the FIR line emission. The LWS observations provide a good dust temperature estimate; combining this with our previous data allows us to constrain the $N(\mathrm{H_2})/I_{\mathrm{CO}}$ ratio to the range $5\text{–}8 \times 10^{19}\,\mathrm{cm^{-2}(\,K\,km\,s^{-1})^{-1}}$ in the inner disk of this normal spiral.

We present a 10 GHz–10 THz (3 cm to 30 μm) spectrum of the line and continuum emission of the ISM in NGC 4414. To the extent that the frequency ranges overlap, the FIR continuum and spectral line properties of NGC 4414 are similar to the COBE data for the Galaxy. The ISO LWS cannot survey the entire Galaxy but can study single objects such as HII regions or molecular clouds. The sum of the individual features identified by ISO in the Galaxy plus the diffuse gas should yield a spectrum similar to the template presented here. In contrast, the spectrum of NGC 4414 is very different from that of early starbursts such as NGC 4038/9 and Arp 299 and from more evolved starbursts such as Arp 220.

Key words: galaxies: individual: NGC 4414 – galaxies: ISM – galaxies: spiral – infrared: galaxies – radio continuum: galaxies – radio lines: galaxies

Send offprint requests to: Jonathan Braine
(braine@observ.u-bordeaux.fr)

1. Introduction

Until recently, identifying the important cooling lines in the interstellar medium (ISM) of galaxies has been restricted, for reasons of sensitivity, to luminous starburst galaxies (e.g. Carral et al. 1994). Furthermore, complete spectral scans are not possible even from airborne observatories due to the Earth's atmosphere. The Infrared Space Observatory Long Wavelength Spectrometer[1] (ISO LWS; Clegg et al. 1996) gives us the opportunity to measure the FIR emission of weak sources such as ordinary galaxies from 40 to 190 microns with no breaks. Theoretical modelling and observations of the Milky Way and other galaxies (Crawford et al. 1985; Tielens & Hollenbach 1985a; Bennett et al. 1994) show that the strongest cooling lines of the ISM are not the CO lines that dominate the millimeter emission, although these are important for the cool, dense ISM, but lines in the FIR, particularly the CII line at 158 μm.

Observations of the Galaxy provide unique information about individual sources such as HII regions, Photo-dissociation regions (PDRs), molecular clouds,... but developing a face-on view of the Galaxy or even calculating total luminosities from our in-plane observing site is quite complicated. Using COBE data, Wright et al. (1991) fit the FIRAS observations to a 3 component model of the galaxy defined as a central gaussian peak, an exponential disk, and a "molecular" ring with a gaussian radial profile. Bloemen et al. (1990) fit the IRAS 60 and 100 μm to the HI and CO surveys of the Galaxy; they use the HI/CO velocities (assuming rotation curve and circular rotation) to derive distances, average over radial bins a few kpc in size, and assume that the dust emission can be expressed as a linear combination of the HI and CO emission. Sodroski et al. (1994) represent the COBE DIRBE 140 and 240 μm emission from the galactic plane as a linear combination of the HI, CO, and 5 GHz continuum emission to derive FIR emissivities for the molecular, atomic, and ionized gas; these are then multiplied by previous estimates of the mass of each gas component to derive the total FIR luminosity. It is in fact much more difficult to derive global emission characteristics for the Galaxy than for local spirals, where all

[1] Based on observations with ISO, an ESA project with instruments funded by ESA Member States (especially the PI countries: France, Germany, the Netherlands and the United Kingdom) with the participation of ISAS and NASA.

Table 1. Basic information about NGC 4414. $L_{\rm FIR\,total}$ is calculated by integrating the two-temperature fit to the ISO LWS spectrum. H-magnitude (total, not $H_{-0.5}$) estimated from Condon et al. (1987)

RA(1950)	12 23 57.8
Dec(1950)	31 29 58
Distance	9.6 Mpc
$L_{\rm IRAS:40–122\,\mu}$	$5.5\,10^9$ L$_\odot$
$L_{\rm FIR\,total}$	$11\,10^9$ L$_\odot$
$L_{\rm Blue}/L_{\rm B,\odot}$	$8.9\,10^9$
optical/NIR fluxes and mag.	
B (0.44 μm, B_T^0)	10.52 mag, 0.264 Jy
V (0.55 μm)	9.74 mag, 0.487 Jy
U (0.365 μm)	10.63 mag, 0.106 Jy
H (1.65 μm)	6.8 mag, 1.9 Jy

components are at the same distance and no assumptions about the distribution are necessary.

The FIR NII (122 and 205 μm), CII (158 μm), and possibly OI(145 μm) lines were detected in the Galaxy by the COBE FIRAS instrument (Wright et al. 1991; Bennett et al. 1994). Other FIR observations of the Galaxy pinpoint specific regions such as Orion or the Galactic Center with the exception of the unbiased LWS parallel mode observations which detected the OI (63 μm) and CII lines with a preliminary ratio of CII/OI $\approx$ few (Caux & Gry 1997).

We selected NGC 4414 as a good representative of a "normal" galaxy whose emission averaged over the ISO LWS beam should be representative of the inner disk or molecular ring of a spiral such as our own. It is a relatively isolated Sc galaxy near the North Galactic Pole (b=83°). The highly extended ^{12}CO, ^{13}CO, and HI emission (Braine et al. 1997 – hereafter Paper II) shows that no recent interaction with another galaxy has occurred. Furthermore, very little ionized or neutral gas is present in the nucleus (Pogge 1989; Braine et al. 1993 – hereafter Paper I; Sakamoto 1996; Braine et al. in prep.), enabling us to measure the emission of a quiescent galactic disk with minimal contribution from any nuclear emission.

The properties of the neutral ISM in galactic nuclei are different – denser, warmer, non-negligible tidal shear – from those in galactic disks. Given the poor spatial resolution of ISO in the FIR (~ 4 kpc at a distance of 10 Mpc), the LWS beam cannot separate the nuclear and disk emission except for the very closest spiral galaxies. However, due to the absence of CO, HI, or Hα emission in the center of NGC 4414, the FIR emission we detect comes from the disk. We are thus dealing with a simpler system than, say, observations of the centers of NGC 891 or NGC 6946 where the nuclear ISM emits strongly and cannot be separated from disk emission.

At the assumed distance of 9.6 Mpc ($H_0 \approx 75\,{\rm km\,s^{-1}}$ Mpc^{-1}), in keeping with our previous work, the ISO LWS beam ($\sim 80''$ FWHM) corresponds to a galactocentric radius of 2 kpc and closely matches the CO-bright part of the disk of NGC 4414 (see Fig. 2 in Paper I). The most logical comparison is thus with the molecular ring, excluding the nucleus, in the Milky Way. The gas surface density (*i.e.* CO brightness) in this part of NGC 4414 is several times that of the molecular ring of the Galaxy but lower than that of the disk of M 51 or mild/moderate starbursts and orders of magnitude below that of Ultra-luminous IR galaxies. The LWS observations presented here complete the radio-optical spectral energy distribution for this galaxy.

Pre-ISO FIR spectroscopy of galaxies was limited to the CII line except for the local starbursts M 82 and NGC 253 and the IR-luminous merger NGC 3256. ISO LWS spectral scans have been presented for NGC 4038/9 (Fischer et al. 1996), Arp 299 (Satyapal et al. 1998), Circinus (Genzel 1997), Arp 220 (Fischer et al. 1997), and the major lines were observed in NGC 5713 by Lord et al. (1996a). All of these galaxies are more actively forming stars than NGC 4414. Furthermore, the emission cannot be interpreted as coming from a more-or-less quiescent disk due to the nuclear or starburst components. The other (unpublished) LWS spectral scans of galactic disks were made with much lower integration times (factor 3–8) than what we present here.

The goal of the LWS observations of NGC 4414 is to derive cooling rates and dust temperatures, thereby providing a high-quality template for the FIR emission of the ISM, integrated over several kpcs, of a "normal" spiral disk.

2. Observations and reduction

NGC 4414 was observed with ISO LWS on July 3 1996, centered at 12:23:57.8, 31:29:58 (B1950), for 6183 seconds using the LWS01 fast-scanning mode with 8.5 sec. integration per step and a spectral sampling interval of 8. An off-position 5 arcmin. East was observed for 1175 seconds using the LWS01 fast-scanning mode with 5 sec. integration per step and a spectral sampling interval of 2.

The LWS Standard Processed Data (SPD) were reduced using the LWS Interactive Analysis software (LIA[2]). Dark currents, estimated from calibration observations, were subtracted and corrections for drifts in the detector responsivity were applied. The overlapping wavelength coverage between the 10 LWS detectors was used to adjust their relative calibration and the absolute calibration was normalised to that of detector LW1 (83–114 μm).

3. Results and analysis

The entire LWS spectrum from $43\,\mu{\rm m} - 189\,\mu$m, for both the on and off-source positions, is shown in Fig. 1. No significant emission is detected in the off-position, in agreement with the COBE non-detection of CII(158 μm) at such high galactic latitudes (Bennett et al. 1994). The spectral scan at the off-source position shows greater noise, due to the shorter integration time, than the on-source spectrum. However the off-source observation still achieved its objective, which was to demonstrate

[2] The ISO LWS data presented in this paper was analysed using the LWS Interactive Analysis Software (LIA), developed by RAL and IPAC (see Sidher et al. 1998). The ISO Spectral Analysis Package (ISAP) is a joint development by the LWS and SWS Instrument Teams and Data Centers. Contributing institutes are CESR, IAS, IPAC, MPE, RAL and SRON.

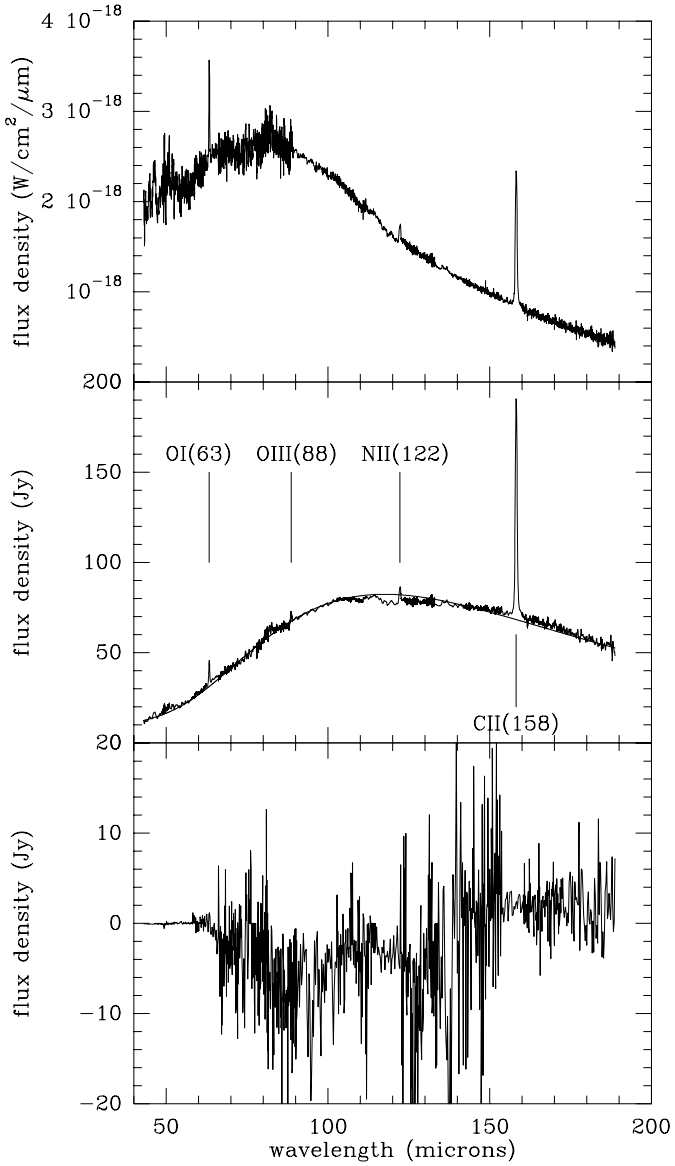

Fig. 1. ISO LWS spectrum of NGC 4414 (*top* and *middle*) and off position (*bottom*) with all detectors averaged. Middle panel shows two-temperature dust emission (69 K and 24.5 K) scaled to 25 μm and 245GHz continuum observations as solid line over spectrum. We show the flux density of NGC 4414 both in Jy and in Watts/cm^2/μm to aid the comparison with other data.

that the local ISM does not contaminate the FIR spectrum of NGC 4414.

As a check of the flux calibration, we calculated the continuum flux through the IRAS 60 and 100 μm passbands. The LWS "60 μm" and "100 μm" fluxes are 31.5 Jy and 76 Jy respectively, and are within 10% of the IRAS Addscan flux densities, 31.5 Jy and 70 Jy (Young et al. 1989). We do not consider the difference in ISO LWS and IRAS calibration at 100 μm to be significant. There remain small differences, particularly at ~ 120 μm, in the relative calibration of the individual LWS detectors. However these are minor calibration uncertainties and as such do not affect the conclusions of this paper. Odenwald et al. (1998) compared galaxy fluxes determined by IRAS and through COBE DIRBE observations and found, as we here for ISO LWS, that while the 60 μm flux was about equal to the IRAS flux, the 100 μm IRAS fluxes were lower (by up to 20–30% compared to DIRBE). The favorable comparison to these data and the excellent fit to grey-body thermal dust emission curves (next section) suggests that the fluxes presented here are calibrated to better than about 15%.

3.1. Dust continuum emission

While necessarily an oversimplification, even for a galactic disk, we model the FIR spectral energy distribution with thermal emission from a cool and warm dust component and a single emissivity law. The ISO LWS grating-scan provides full spectral coverage of the FIR regime, and consequently a much greater constraint on the temperature of the dust emission than the previous IRAS 25 μm, 60 μm and 100 μm flux densities.

We assume that the warm component produces the IRAS 25 μm emission and that the cool component generates the $1.2\,\mathrm{mm}$ flux detected in Paper II. The resolved mm-continuum emission contributes $\sim 0.16\,\mathrm{Jy}$ in an 80″ aperture (LWS beam FWHM) centered on the galaxy nucleus. The total IRAS addscan 25 μm flux density is $3.6\,\mathrm{Jy}$. To model the dust emission, we take $F_\lambda \propto \epsilon_\lambda B(\lambda, T)$, where $\epsilon_\lambda = 1 - exp(-25\,\mu^2/\lambda^2)$, which is a continuous function leaving a "standard" ν^2 (*i.e.* $\beta = 2$) emissivity at longer wavelengths and is very similar to the wavelength dependence derived by Draine & Lee (1984).

The dust temperatures of the two component model which yield the continuum emission shown in Fig. 1 (middle panel) are 69 and 24.5 K. The cool dust temperature is substantially warmer than the $15\,\mathrm{K}$ we assumed for the cool component in Paper II, although LWS only observes the warmer inner galactic disk of NGC 4414. A lower dust temperature of $\sim 15\,\mathrm{K}$ may well be appropriate for the outer disk (*cf.* Sect. 3.4).

Assuming a grain cross-section of $\sigma_\lambda = 10^{-26}\mathrm{cm}^2\lambda_{\mathrm{mm}}^{-2}$ per H-nucleus (e.g. Krügel & Chini 1994; Pollack et al. 1994), we calculate gas masses of $M_{\mathrm{cool\,gas}} \approx 7 \times 10^8\,\mathrm{M}_\odot$ and $M_{\mathrm{warm\,gas}} \approx 6 \times 10^5\,\mathrm{M}_\odot$ (including Helium) within the LWS beam. This cross-section is a factor 1.45 greater than that of Draine & Lee (1984). It should be noted that cooler material ($\mathrm{T} < 20\,\mathrm{K}$), which does not contribute significantly to IRAS fluxes, is present at larger radii so this is not the total gas mass of NGC 4414 (*cf.* Sect. 3.4).

The gas mass we derived from our HI, ^{12}CO, and ^{13}CO observations (Paper II) was about $M_{\mathrm{gas}} \approx 1.2 \times 10^9\,\mathrm{M}_\odot$ within the LWS beam, using a mean $N(\mathrm{H}_2)/I_{\mathrm{CO}(1-0)}$ value of about $1.1\,10^{20}\,\mathrm{cm}^{-2}(\,\mathrm{K\,km\,s}^{-1})^{-1}$ derived from comparison between ^{12}CO(1–0) and the ^{12}CO(2–1), ^{13}CO(1–0), ^{13}CO(2–1), and 1.2 mm continuum. If this mass were correct, then the average grain cross-section within the LWS beam would be less than that derived by Draine & Lee. It is more likely that in 1997 we overestimated the gas mass because (1) at the time no temperature information was available and we assumed $T_{dust} \sim 15\,\mathrm{K}$ and (2) we used the average of the ^{13}CO

column densities provided by the ^{13}CO(1–0) and ^{13}CO(2–1) measurements – the ^{13}CO(2–1) is probably a better estimate. If we adopt the gas mass of $7 \times 10^8\,\mathrm{M}_\odot$ for the central $80''$ of NGC 4414, the average CO-H_2 conversion factor is about $N(\mathrm{H}_2)/I_{\mathrm{CO}(1-0)} \approx 0.5 \times 10^{20}\,\mathrm{cm}^{-2}(\,\mathrm{K\,km\,s}^{-1})^{-1}$.

Errors in the dust and gas masses vary linearly with the grain cross-section, which is unlikely to be wrong by more than a factor ~ 2 averaged over large area ($\sim 11\,\mathrm{kpc}^2$) given the mixture of conditions present. The temperature uncertainties are strongly dominated by the emissivity law. We fit Hildebrand's (1983) discontinuous emissivity law and find a "cool" dust temperature of 30.5 K. A $\beta = 1.5$ emissivity-law, where $F_\nu \propto \nu^\beta B(\nu, T)$, and a cool dust temperature of 27.5 K fits as long as the frequency dependence of the dust emissivity steepens to $\beta \approx 2$ for wavelengths $\lambda \gtrsim 250\,\mu$m in order to fit the 1.2 mm data point.

For the same cross-section, these different temperatures, 30.5 K and 27.5 K, yield gas masses a factor 3 and 2, respectively, lower than the cold component (24.5 K) included in the model shown in Fig. 1. In all cases, the warm component is less than 1% of the mass.

A large data set consistently points to a $N(\mathrm{H}_2)/I_{\mathrm{CO}(1-0)}$ ratio of order 0.5–$0.8 \times 10^{20}\,\mathrm{cm}^{-2}(\,\mathrm{K\,km\,s}^{-1})^{-1}$ for the inner disk of this normal galaxy. The $\beta = 1.5$ or Hildebrand emissivities would yield still lower values which are very difficult to reconcile with our ^{12}CO and ^{13}CO observations (M_{gas} close to M_{HI}). The complete LWS scan provides strong constraints on the dust temperature. The other crucial dust measurement, however, is our earlier 1.2 mm map which allows us to exclude a massive cool component, undetectable by the LWS, in the inner disk. If the total uncertainty in the 1.2 mm measurement is up to 30%, then, if the inner disk 1.2 mm flux density were raised by 30%, a cool component could then be present which would raise the gas mass to $10^9\,\mathrm{M}_\odot$. We estimate the neutral gas mass of the inner disk of NGC 4414 to be in the range 0.7–$1 \times 10^9\,\mathrm{M}_\odot$, yielding the above $N(\mathrm{H}_2)/I_{\mathrm{CO}}$ factor. These data suggest that the mass of the molecular ring in the Milky Way may be overestimated as well.

3.2. Spectral line emission

The OI(63 μm), NII(122 μm), and CII(158 μm) lines are obviously well detected in Fig. 1. The rest-frame wavelengths, line fluxes and luminosities are given in Table 2. The OIII(88 μm) line is visible in both detectors 4 and 5 and the flux given in Table 2 is the average with the uncertainty reflecting the difference. The OI(146 μm) line may be detected at a very low level which is given in Table 2 as well. In Figs. 2 and 3 we show the individual spectra of these lines after subtracting our two-component model to the dust continuum. No unexpected strong lines are present in the spectrum.

Where does the line emission come from? No consensus is reached for the Galaxy – PDRs (Tielens & Hollenbach 1985a – hereafter TH85a), the cold neutral medium (CNM; Bennett et al. (1994), the extended low-density warm ionized medium (ELDWIM; Heiles 1994), and perhaps even HII regions (Gry et al. 1992) have been cited as major sources for the CII line emission. It must be stressed that the three reliable line fluxes (CII, NII, and OI) and one other detection (OIII) are absolutely not sufficient to derive the physical conditions over the several kpc^2 of the ISO beam. The present observations nonetheless provide substantial and currently unique information about the global emission of a spiral disk which is not available for the Milky Way, where data for many individual galactic sources are available. In the following, the CNM refers to atomic and molecular clouds and their edges and by ELDWIM we mean the diffuse ionized gas of all sorts. All neutral clouds have surfaces and are surrounded by ionized gas so it appears inevitable that neutral clouds have some photodissociated gas. Furthermore, we now know that the clumpy nature of clouds creates pockets of photo-dissociated gas deep into molecular and atomic clouds (e.g. Boissé 1990) and this material belongs to the CNM. PDR, as used here, refers to a region exposed to a strong UV field generated locally in conjunction with an HII region (Fig. 1 in TH85a) such as in Orion (Tielens & Hollenbach 1985b).

The NII emission comes from ionized gas, unlike the CII (the ionization potential of carbon is lower than that of hydrogen so the carbon can be ionized while the H remains largely neutral – this is not the case for oxygen or nitrogen). The OI 63 and 145 μm lines are respectively from levels 228 and 326 K above the ground state and require high densities to be ex-

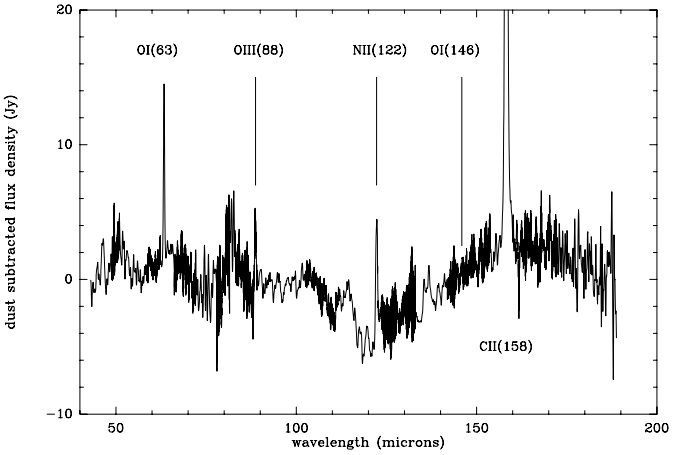

Fig. 2. ISO LWS spectrum of NGC 4414 with model of dust continuum subtracted.

Table 2. Lines detected in NGC 4414; wavelengths are laboratory rest wavelengths. Uncertainties are intended to include calibration and rms noise.

Line	transition	wavelength μm	flux $10^{-19}\,\mathrm{W\,cm}^{-2}$	Lum. $10^6\,\mathrm{L}_\odot$
CII	$2p:^2p_{3/2}-^2p_{1/2}$	157.741	10.6 ± 2	31
OI	$2p^4:^3p_0-^3p_1$	145.526	$\lesssim 0.1$	$\lesssim 0.3$
NII	$2p^2:^3p_2-^3p_1$	121.897	1.3 ± 0.4	4
OIII	$2p^2:^3p_1-^3p_0$	88.356	1 ± 0.5	3
OI	$2p^4:^3p_1-^3p_2$	63.1837	3.3 ± 1	10

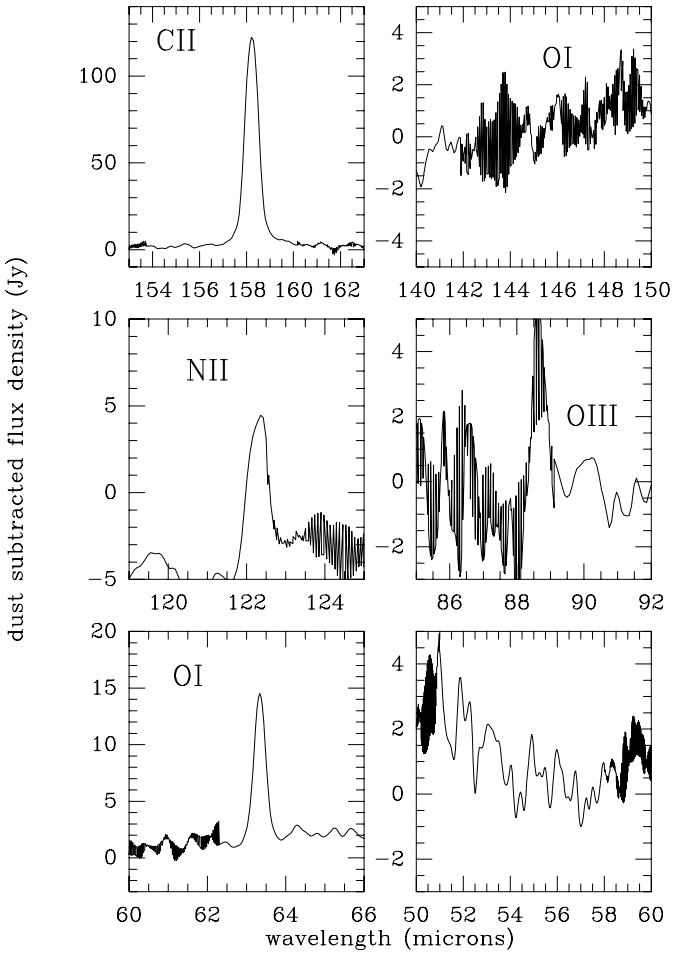

Fig. 3. Individual lines in ISO LWS spectrum of NGC 4414 with model of dust continuum subtracted, which is why the base of the line is not always at zero. At some wavelengths two detectors overlap; the thickness of the black area indicates the difference between the two datasets. The last panel shows the region covering the undetected OIII(52) and NIII(57) lines.

cited. The IR line cooling of HII regions is dominated by the OIII 52 and 88 μm lines except for the lowest effective stellar temperatures (Rubin 1985). CII is not a major coolant of such HII regions. The IR line cooling in standard PDRs and PDR/HII regions is dominated by OI (63 μm) followed by the CII and OI 145 μm lines (TH85a,b; Hermann et al. 1997) with $L_{\rm CII}/L_{\rm FIR} \approx 10^{-4} - 10^{-3}$, an order of magnitude lower than in galaxies (e.g. Stacey et al. 1991).

Let us start with OI. OI emission is from neutral gas but combines with C or O to form CO or O_2 when shielding is sufficient (Fig. 1 of TH85a). The OI 63 and 145 μm lines come from PDRs and the observed intensity ratio OI$(63/145) \gtrsim 30$ is in agreement with a wide range of parameters for the TH85a PDRs. In Orion and in the young Planetary Nebula NGC 7027 I(OI 63)/(CII 158)$\sim$ 10 and OI 145 μm is somewhat weaker (factor $\lesssim 2$) than CII (TH85b; Hermann et al. 1997; Liu et al. 1996), close to the standard model in TH85a. We may reasonably attribute 3–10% of the CII emission in NGC 4414 to classical PDR/HII regions.

The OIII emission comes from classical HII regions but not from the ELDWIM. The OIII (88 μm) line is typically stronger than the NII emission from HII regions so while some of the NII flux comes from HII regions, most of the NII is from the ELDWIM. This is the case in the Galaxy (Bennett et al. 1994; Heiles 1994) where both the NII 122 μm and 205 μm lines were detected (Wright et al. 1991). The Galactic OIII emission has not been measured.

The density, or distribution of densities, of the diffuse ionized gas is unknown but is certainly below the critical density for the NII lines. This means that the emission per NII ion varies directly with the unknown volume density. From the Galactic CII/NII(205) intensity ratio, Heiles (1994) argues that the ELDWIM could be the major source of CII emission but stresses that large uncertainties, including uncertainties in collisional cross-sections (Heiles 1994; Osterbrock 1989), are present. In the low density limit, and assuming that all of the NII emission comes from the ELDWIM, the ELDWIM could account for all of the CII emission detected in NGC 4414, just as in the Galaxy. This shows that the ELDWIM may well be an important contributor but also that the low-density limit is probably not appropriate. The CII/NII ratio decreases as the density of the ELDWIM increases. Two factors, however, suggest that the CNM is an important, and probably the most important, source of CII emission. Firstly, the cooling rates estimated for the CNM (Wolfire et al. 1995; Boulanger et al. 1996) provide for 20 – $\gtrsim$ 80% of the CII emission from NGC 4414. Secondly, CII emission clearly increases with star formation activity (e.g. Crawford et al. 1985), although imperfectly, whereas LWS spectra of galaxies show that NII emission is weak in starbursts. Were the CII and NII coming from the same gas (the ELDWIM), then actively star-forming galaxies with strong CII emission like NGC 4038/9, Circinus, NGC 5713, and Arp 299 would not have such weak (or undetected) NII 122 μm lines (see next section). Nonetheless, Heiles' point is well taken – the ELDWIM contribution to the CII flux could equal that of the CNM.

Considering only the flux in the IRAS 60 and 100 μm bands, the $L_{\rm CII}/L_{\rm FIR}$ ratio is 0.0055 in NGC 4414, which places it in the normal range for spiral galaxies (Stacey et al. 1991; Malhotra et al. 1997). Integrating over the entire spectrum, $L_{\rm CII}/L_{\rm FIR} \sim 0.003$, as in the Galaxy (Wright et al. 1991). Similarly, the CII/CO(1–0) luminosity ratio is about 1600 within the LWS beam, close to the average value for the non-starburst galaxies in Stacey et al. (1991).

3.3. Comparison of NGC 4414 with other galaxies

LWS spectra have been presented for the following galaxies – NGC 4038/8, Circinus, Arp 299, Arp 220, and NGC 5713 observed with ISO LWS and NGC 253 and NGC 3256 observed by Carral et al. (1994) with the KAO. A more heterogeneous set of observations of these lines is also available for the central area of M 82 (Lord et al. 1996b).

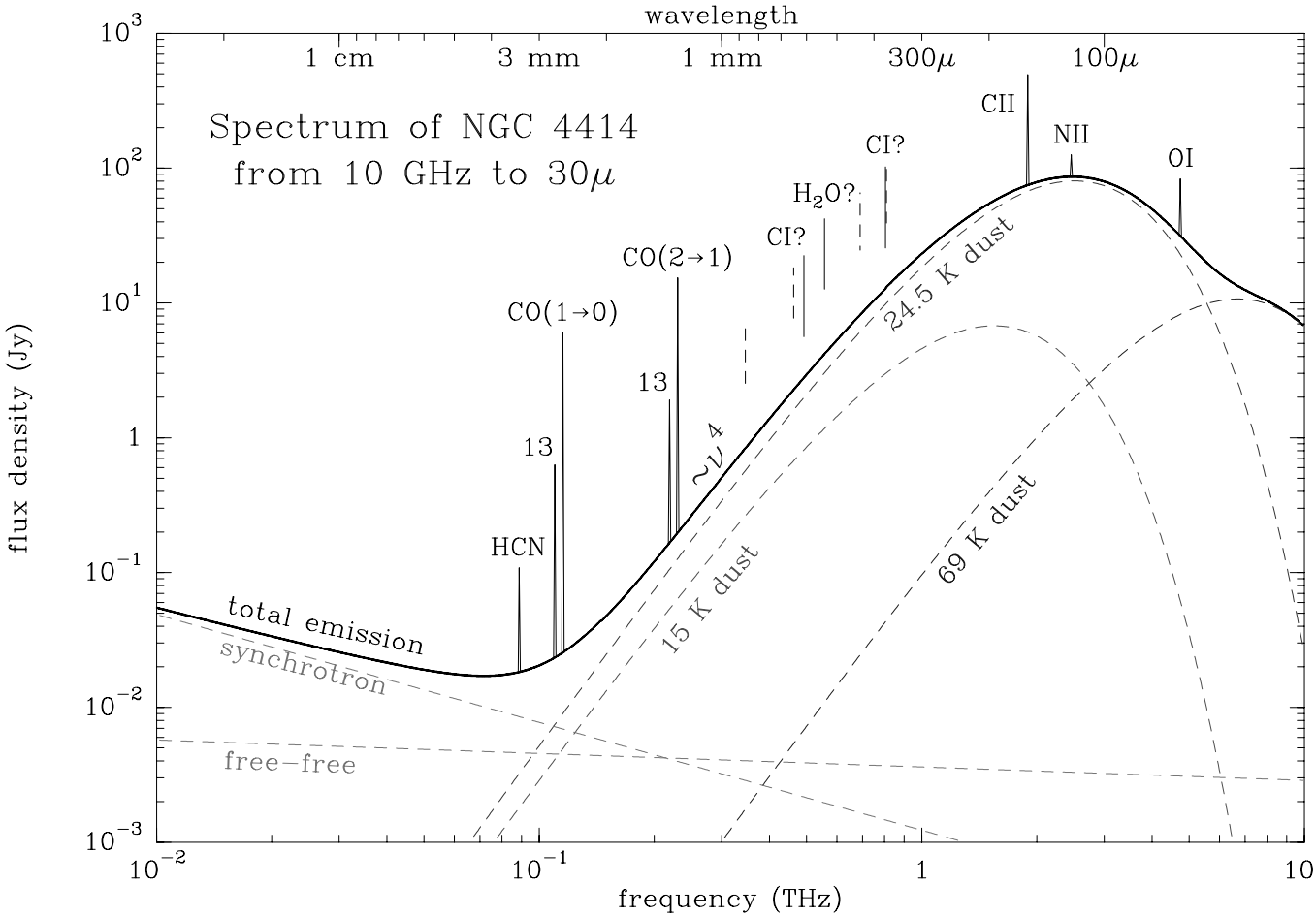

Fig. 4. Global radio – far-infrared spectrum of NGC 4414 including breakdown into emission processes. The CI, H_2O, and high-J CO lines (indicated by vertical dashed lines) have not yet been observed.

All of these galaxies are more actively forming stars than NGC 4414. In the strong starbursts NGC 4038/9 and Arp 299, the strong lines are OIII 52, 88 μm, OI 63 μm, and CII 158 μm and the NII line is not detected. In the milder starbursts NGC 5713 and Circinus, CII is the strongest line followed by OI 63 μm and OIII 88 μm but NII is weak. The KAO observations of NGC 253 and NGC 3256 seem to place both galaxies in an intermediate case – equally strong CII and OI 63 μm and detected OIII but no NII observations were made. The spectrum of Arp 220 is dominated by absorption lines, presumably due to the small warm optically thick nucleus (Downes et al. 1993). The line strengths in the center of M 82 fit into the strong starburst class above. The NII lines are detected in M 82 but the NII (122/205) line ratio (~ 4 as opposed to ~ 1 in the Galaxy) suggests that the emission is from HII regions rather than the ELDWIM.

The observations described above fit into the framework where the high UV field and abundant molecular gas in starburst galaxies creates more dense PDR and HII regions. There is no evidence for a decrease in NII luminosity in starbursts because the NII 122 μm luminosity of NGC 4414 (or the Galaxy), if placed at the distance of NGC 5713, NGC 4038/9, or Arp 299, would not be detected in those spectra. While the NII/CII intensity ratio appears to decrease with increasing levels of star formation, the current observational uncertainties are such that this is not a strong limit to the fraction of CII emission coming from the same (ELDWIM) gas as the NII (see preceding section).

It is worth noting that published line fluxes are not available for Arp 299 or Circinus, NII was not observed in NGC 253 and NGC 3256, and the calibration of some of the lines in NGC 5713 is subject to caution (Lord et al. 1996a). The NGC 4414 data presented here are a unique data set.

3.4. A template for the emission of a galactic disk

The goal of this work is to provide a high-quality template for the global emission of the ISM of a galactic disk. We present the 10 GHz–10 THz (3 cm to 30 μm) spectrum of NGC 4414 in Fig. 4 along with a likely decomposition into physical processes. All data are for the entire disk except the LWS spectral lines but the emission at LWS wavelengths in the outer disk is probably very low. The cm-wave part is a fit to points in Duric et al. (1988) and Niklas et al. (1995). The mm-wave data are from Papers I

and II and the FIR from this paper. Spectral lines have been averaged over a line width of $400\,\mathrm{km\,s^{-1}}$. The cool (24.5 K) and warm (69 K) dust spectra are from the LWS spectrum in Fig. 1. The CI, H_2O, and high-J CO lines (indicated by vertical dashed lines) and the submm continuum have not yet been observed.

We dispose of the following data for the thermal dust continuum: IRAS wideband 100, 60, and 25 μm whole-galaxy fluxes; ISO LWS spectrum covering the central $80''$; and a map at 1.2 mm with a resolution of $11''$. A coherent picture can be obtained from these data. (a) The IRAS and LWS flux densities agree, showing that ISO detected all of the cool/warm dust in NGC 4414 – *i.e.* the dust contributing to the IRAS measurements ($T \gtrsim 25$ K) is within the $80''$ ISO LWS beam. (b) The 1.2 mm flux within the LWS beam is accounted for naturally by our fits to the LWS spectrum (24.5 and 69 K curves in Fig. 4) so no dust cooler than 24 K is required to fit the 1.2 mm flux within the LWS beam. (c) Substantial 1.2 mm flux is detected outside the ISO LWS beam yet the agreement between the ISO and IRAS flux densities at 100 and 60 μm shows that this outer disk material does not contribute measurably to the IRAS fluxes – the source of the emission is cold dust ($T < 20$ K), represented by the 15 K dust curve in Fig. 4. The temperature of the cold dust is not well constrained – detected at 1.2 mm but not at 100 μ by IRAS – but 15 K is a very plausible temperature.

What does the cold dust curve signify? Even at the longest wavelengths of the LWS, the emission from this component is $\lesssim$ 10% that of the warmer dust and such fluxes are within calibration uncertainties. Yet the gas mass associated with this cold component is about the same as that of the warmer (24.5 K) dust and perhaps even slightly greater because the metallicity is probably lower in the outer disk so a lower dust emissivity would be appropriate. This massive component is *not* present in the LWS beam because the 24.5 K dust provides all the flux observed within the ISO LWS beam at 1.2mm.

Fig. 4 may provide the best image to date of what the spectrum of the molecular ring of our Galaxy would look like if observed from another galaxy.

4. A look forward

In this paper we have presented a full spectral scan from 43 to 189 microns of what could reasonably be considered a normal galactic disk. It is likely that this is what an outside observer would obtain when looking at the molecular ring in our galaxy, without all the problems (being blinded by local material and unable to derive a face-on view of our disk) we have when observing our galaxy from within its thin disk.

The problem in obtaining the global spectrum of the Galaxy can be illustrated as follows. Two roughly co-eval CO(1–0) surveys of the Milky Way (Sanders et al. 1984; Dame & Thaddeus 1985) obtained quite different results for the H_2 mass of the Galaxy. Most of the difference is *not* due to different $N(H_2)/I_{CO}$ factors (Bronfman et al. 1988) but rather to derived CO luminosities. Using the COBE FIRAS instrument, the luminosities in the CO lines estimated by Wright et al. (1991) are much lower than either previous estimate. Bennett et al. (1994) point out that Wright et al. underestimate the CO luminosities because they assumed that the CO/FIR ratio was constant. In fact, the CO is more centrally peaked and this effect increases with J. Velocity information is not available to help determine more accurate luminosities for this unique survey of CO lines. If the Galactic CII/CO(2–1) luminosity ratio is really ~ 300, as in NGC 4414, then Wright et al. underestimated the CO(2–1) luminosity by a factor 2 (if $L_{\rm CII}$ is correct) due to the uncertainty in the distribution of the emission.

It is important to address the issue of high-J CO lines because of the increasing number of IR-luminous objects, usually gravitationally lensed, detected in high-J CO lines redshifted to mm wavelengths. Will we be able to detect normal galaxies, if they exist, at high redshift? Solomon et al. (1992) pointed out that the CO line intensity varies as $I_{\rm CO} = L'_{\rm CO}(1+z)^3/(\Omega_b D_L^2)$ where D_L is the luminosity distance and $L'_{\rm CO}$ is the CO luminosity in brightness units ($\mathrm{K\,km\,s^{-1}\,pc^2}$). At a given telescope and frequency, the beam size Ω_b stays constant and $I_{\rm CO}$ should not decrease with increasing redshift because $(1+z)^3/D_L^2$ increases slowly with z, making it much easier than expected to detect CO in distant objects by observing successively higher transitions as one goes to higher redshift objects. An important caveat, however, is the constant $L'_{\rm CO}$ hypothesis. The Wright et al. data indicate that for the Milky Way $L'_{\rm CO} \propto \nu^{-3}$ for $J \geq 2$ (constant luminosity in $\mathrm{L_\odot}$). Such a steep decrease appears unreasonable but underlines how little we know about $J > 3$ CO transitions in normal galaxies. The answer conditions whether we will be able to detect high-redshift "normal" galaxies *or* prove they do not exist.

Our data (Fig. 4) should be considered a template for the large-scale emission of a disk. As such, they are complementary to Galactic observations where good linear resolution is available, enabling individual molecular clouds and HII regions to be studied, but where we are too sensitive to local material to be confident of the overall picture. The continuing improvements in models and observations and the ever-increasing wavelength coverage will yield more precise images of the emission of the various components of the ISM in our galaxy – PDRs, CNM, ELDWIM... The NGC 4414 data can be viewed as the sum of all these over large areas and the respective masses in each phase of the ISM will become clearer as our knowledge of the individual components improves.

After the LWS observations, the main gap in our knowledge of the emission of the ISM is the submm from 1 mm to 200 μm (see Fig. 4). CI (492 GHz) is the next most important coolant of the neutral ISM and necessary in any template. High-J CO observations would show whether an observable amount of very dense warm gas is present, much like Harris et al. (1991) for starburst nuclei. With ground-based sub-mm telescopes offering beam-sizes of $\sim 11''$ at 492 GHz and nearby galaxies like NGC 4414, it is possible to measure the CI/CO ratio as a function of radius and follow up earlier observations of the CO($\frac{2-1}{1-0}$) line ratio in NGC 4414 (Paper II). The CI line is optically thin so it provides an estimate of the neutral carbon column density which can be compared with our existing CO, ^{13}CO, HI, and dust continuum measurements – does the fraction of atomic

carbon increase as the gas temperature, abundance, and radiation field decrease with galactocentric distance? The high-J CO lines come from the same warm dense regions as the OI 63 μm emission (HII/PDR/molecular cloud interfaces) and the CI from the more diffuse photo-dissociated gas which emits strongly in the CII line. The relative strengths of the CI and high-J CO lines provide one of the clearest means of separating the dense and diffuse PDR components both as a function of radius and integrated over the disk.

Acknowledgements. We thank Sunil Sidher and Sarah Unger for their assistance in the reduction of these LWS data.

References

Bennett C.L., Fixsen D.J., Hinshaw G., et al., 1994, ApJ 434, 587
Bloemen J.B.G.M., Deul E.R., Thaddeus P., 1990, A&A 233, 437
Boissé P., 1990, A&A 228, 483
Boulanger F., Abergel A., Bernard J.-P., et al., 1996, A&A 312, 256
Braine J., Combes F., van Driel W., 1993, A&A 280, 451 (Paper I)
Braine J., Brouillet N., Baudry A., 1997, A&A 318, 19 (Paper II)
Bronfman L. Cohen R.S., Alvarez H., May J., Thaddeus P., 1988, ApJ 324, 248
Carral P., Hollenbach D.J., Lord S.D., et al., 1994, ApJ 423, 223
Caux E., Gry C., 1997, In: Wilson A. (ed.) The ESA Symposium: The Far InfraRed and Submillimeter Universe. ESA, Noordwijk, p. 67
Clegg P.E., Ade P.A.R., Armand C., et al., 1996, A&A 315, L38
Condon J.J., Yin Q.F., Burstein D., 1987, ApJS 64, 543
Crawford M.K., Genzel R., Townes C.H., Watson D.M., 1985, ApJ 291, 755
Dame T.M., Thaddeus P., 1985, ApJ 297, 751
Downes D., Solomon P.M., Radford S.J.E., 1993, ApJ 414, L13
Draine B.T., Lee H.M., 1984, ApJ 285, 89
Duric N., Bourneuf E., Gregory P.C., 1988, AJ 96, 81
Fischer J., Shier L., Luhman M.L., et al., 1996, A&A 315, L97
Fischer J., Satyapal S., Luhman M.L., et al., 1997, In: Heras A.M., Leech K., Trams N.R., Perry M., First ISO Workshop on Analytical Spectroscopy. ESA SP-419, ESA Publications Division, p. 149
Genzel R., 1997, In: Wilson A. (ed.) The ESA Symposium: The Far InfraRed and Submillimeter Universe. ESA, Noordwijk, p. 97
Gry C., Lequeux J., Boulanger F., 1992, A&A 266, 457
Harris A.I., Stutski J., Graf U.U., et al., 1991, ApJ 382, L75
Heiles C., 1994, ApJ 436, 720
Herrmann F., Madden S. C., Nikola T., et al., 1997, ApJ 481, 343
Hildebrand R.H., 1983, QJRAS 24, 267
Krügel E., Chini R., 1994, A&A 287, 947
Liu X.-W., Barlow M.J., N-Q-Rieu, et al., 1996, A&A 315, L257
Lord S.D, Malhotra S., Lim T., et al., 1996a, A&A 315, L117
Lord S.D., Hollenbach D. J. Haas M.R., et al., 1996b, ApJ 465, 703
Malhotra S., Helou G., Stacey G., et al., 1997, ApJ 491, L27
Niklas S., Klein U., Braine J., Wielebinski R., 1995, A&AS 114, 21
Odenwald S., Newmark J., Smoot G., 1998, ApJ 500, 554
Osterbrock D.E. 1989, Astrophysics of Gaseous Nebulae and Active Galactic Nuclei. University Science Books, Mill Valley, CA
Pogge R., 1989, ApJS 71, 433
Pollack J.B., Hollenbach D., Beckwith S., et al., 1994, ApJ 421, 615
Rubin R.H., 1985, ApJS 57, 349
Sakamoto K., 1996 ApJ 471, 173
Sanders D.B., Solomon P.M., Scoville N.Z., 1984, ApJ 276, 182
Satyapal S., et al., 1998, submitted to ApJ
Sidher S.D., et al., 1998, Proc. First ISO Workshop on Analytical Spectroscopy, 6–8 OCt. 1997, (ESA SP-419) p. 297
Sodroski T.J., Bennett C., Boggess N., et al., 1994, ApJ 428, 638
Sodroski T.J., Odegard N., Dwek E., et al., 1995, ApJ 452, 262
Solomon P.M., Radford S.J.E., Downes D., 1992, Nat 356, 318
Stacey G.J., Geis N., Genzel R., et al., 1991, ApJ 373, 423
Tielens A.G.G.M., Hollenbach D., 1985a, ApJ 291, 722
Tielens A.G.G.M., Hollenbach D., 1985b, ApJ 291, 747
Wolfire M.G., Hollenbach D., McKee C.F., Tielens A.G.G.M., Bakes E.L.O., 1995, ApJ 443, 152
Wright E.L., Mather J.C., Bennett C.L., et al., 1991, ApJ 381, 200
Young J.S., Xie S., Kenney J.D.P., Rice W.L., 1989, ApJS 70, 699